Revista Brasileira de Geomorfologia

v. 23, nº 4 (2022)

http://dx.doi.org/10.20502/rbg.v23i4.2151

https://rbgeomorfologia.org.br/rbg
ISSN 2236-5664

Research paper

Controlling factors and mapping of Linear Erosive Features in Santa Maria river watershed –RS

Fatores controladores e mapeamento de feições erosivas lineares na bacia hidrográfica do Rio Santa Maria – RS

Carina Petsch [1], Anderson Augusto Volpato Sccoti [2] Luís Eduardo de Souza Robaina [3] Romario Trentin [4]

1 Universidade Federal de Santa Maria, Santa Maria, RS, Brasil. carinapetsch@gmail.com
ORCID:https://orcid.org/0000-0002-1079-0080
2 Universidade Federal de Santa Maria, Santa Maria, RS, Brasil. asccoti2@gmail.com
ORCID:https://orcid.org/0000-0001-8667-0432.
3 Universidade Federal de Santa Maria, Santa Maria, RS, Brasil. lesrobaina@yahoo.com.br
ORCID:https://orcid.org/0000-0002-2390-6417.
4 Universidade Federal de Santa Maria, Santa Maria, RS, Brasil. romario.trentin@gmail.com
ORCID:https://orcid.org/0000-0002-0615-2801.

Received: 04/08/2021; Accepted: 18/08/2022; Published: 01/10/2022

Abstract: Water erosion is one of the main causes of soil degradation and linear erosion mapping is one of the essential tools for its monitoring. In light of this, the goal from this research is to map the linear erosive features (LEF) of the Santa Maria River Basin (BHRSM), southwest region of RS, and understand which environmental factors are controlling or triggering erosion. In western RS there is a considerable concern associated with erosive processes that occupy large extensions and cause changes in the dynamics of use and changes in the environment. Data on geology, soils, hypsometry, slope, land use, drainage channels and roads were analyzed in a GIS environment. The erosive processes in BHRSM are inherent to the less consolidated sandy substrate, configuring a natural process. The relief energy for the incision of water flows is meaningful, since the LEF are related to moderate slope in portions of medium altitudes. However, anthropogenic action accelerates erosive processes. It is noteworthy that the increase in the area occupied by crops, doubled in the period of 20 years, configuring a new landscape and dynamics for BHRSM, demanding special attention to this region that tends to intensify the erosivy processes.

Keywords: erosion mapping; Google Earth images; southwestern Rio Grande do Sul.

Resumo: A erosão hídrica é uma das principais causas de degradação do solo e o mapeamento da erosão linear é uma das ferramentas essenciais para o seu monitoramento. Diante disso, o objetivo desta pesquisa é mapear as feições erosivas lineares (FEL) da bacia hidrográfica do Rio Santa Maria (BHRSM), sudoeste do RS, e compreender quais fatores ambientes são controladores ou desencadeadores da erosão. No oeste do RS há uma considerável preocupação associada a processos erosivos que ocupam grandes extensões e causam alterações na dinâmica do uso e alterações do meio. Os dados de geologia, solos, hipsometria, declividade, vertentes, uso da terra, canais de drenagem e estradas foram analisados em ambiente SIG. Os processos erosivos na BHRSM são inerentes ao substrato arenoso pouco consolidado, configurando um processo natural. A energia de relevo para a incisão dos fluxos hídricos é significativa, visto que as FEL estão relacionadas às declividades moderadas em porções de altitudes médias. Contudo, a ação antrópica acelera os processos erosivos. Destaca-se que o aumento da área ocupada por lavouras, dobrou no período de 20 anos, configurando uma nova paisagem e dinâmica para a BHRSM, demandando atenção especial para esta região que tende a intensificar os processos erosivos.

Palavras-chave: mapeamento de erosão; imagens Google Earth; sudoeste gaúcho.

1. Introduction

Water erosion is one of the leading causes of soil degradation and it negatively affects soil structure, water and nutrient retention, organic matter content, and ultimately soil fertility in both developed and developing countries (VALENTIN, 2005; MONTANARELLA et al., 2016). It is therefore highlighted that water erosion is the main responsible for global soil degradation and productivity declines (WEI et al., 2017), generating economic losses all over the planet (RAHMATI et al 2016). Sartori et al. (2019) have sought to estimate just the economic impact of soil water erosion on the world economy and the value is estimated at an annual cost of $8 billion to global GDP (Gross Domestic Product). Above all, linear soil erosion represents a significant process of sediment material removal and transport, accounting for 10 to 94% of sediment loss from a watershed (POESEN et al., 2003).

Linear erosion mapping is one of the most essential tools to control this phenomenon, aiming at monitoring land degradation and studying its current and future local impacts (DESPRATS et al., 2013; LIU et al., 2016; AGHARAZI et al., 2017; RAZAVI-TERMEH et al., 2020). Field-based methods were widely used until both aerial photographs and, later, satellite images became available for visual interpretation as well as for applying image processing techniques (SHRUTHI et al., 2015). Aerial photographs, in particular, have been widely used for mapping linear erosive features - LEF - (SIRVIÖ et al., 2004; PELLIKKAA et al., 2005; BOUCHNAK et al., 2009; CONFORTI et al., 2011; OLIVEIRA et al., 2013; BRAGA et al., 2017).

Currently, the satellite images have been used in geomorphological studies for the mapping of landforms, including those resulting from soil erosion (BOARDMAN, 2016) and with the increased availability of high-resolution products, they have become more feasible (SHRUTHI, 2015). Even though these features are easily observed in the field, their small spatial extent usually makes them imperceptible in medium spatial resolution images, which are usually freely available - for instance, images from the Landsat series, with a spatial resolution of 30 meters - (VRIELING, 2006; SHRUTHI et al., 2015).

Since its inception in 2005, the Google Earth (GE) images have been increasingly used in landforms studies (BOARDMAN, 2016), mainly due to its high spatial resolution (BATISTA et al., 2017). According to Boardman (2016), GE can reduce time and expenditures in surveys focused on erosion monitoring. In contemporary soil erosion studies, GE imagery has been surprisingly under-utilized (BOARDMAN, 2016), and is limited to studies identifying gullies, specifically (KARYDAS; PANAGOS, 2020).

Subsequent to Boardman's (2016) work, a few researches are cited that gather efforts for LEF mapping with GE imagery (BRAGA et al., 2017; BATISTA et al; 2018; KNIERIN et al., 2018; KARYDAS; PANAGOS, 2020). Nevertheless, it is emphasized that field work is fundamental for assessing the accuracy of remotely generated products. It is also possible to find in the literature studies in which GE images are used as a support for field mapping (CASTRO et al., 2010; SHRUTHI, 2014) or in multi-sensor analysis (CASTRO et al., 2010) and allied to UAV - Unmanned Aerial Vehicle - images (LIU et al., 2016).

Souza et al. (2017) have emphasized that the literature on studies that relate erosion processes and possible factors that trigger the processes and their characteristics is scarce. Water erosion is controlled by a series of factors that exert influence over the formation and development of linear erosion such as soil type, rainfall erosivity, surface runoff, soil erodibility, soil management, geology, land use, slope gradient slope aspect, curvature, altitude, drainage density, topographic moisture index (TWI), Normalized Difference Vegetation Index (NDVI), distance from roads and soil attributes (pH, clay percentage, electrical conductivity and silt percentage) (VANWALLEGHEM et al., 2005, VALENTIN et al., 2005; VRIELING, 2006; AGNESI et al. 2011; LUCÀ et al., 2011, CUI et al., 2012; EL MAAOUI et al., 2012; SVORAY et al., 2012; SHRUTHI 2014; AMIRI et al 2019).

Some studies have been conducted correlating environmental factors to the presence of LEF (MENÉNDEZ-DUARTE et al., 2007; CASTRO et al., 2010; CONFORTI et al 2011; DESPRATS et al., 2013, BRAGA et al., 2017; KNIERIN et al., 2018; AMIRI et al., 2019; RAZAVI-TERMEH et al., 2020). For Rio Grande do Sul, Rademann et al. (2017) have vectorized the linear features based on GE and related them to lithology. Knierin et al. (2018) associated the LEFs with hypsometry, slope, curvature profiles, curvature planes, and slope shapes.

There have been some studies that have evaluated the erosive processes, either for a single municipality or for the entire Ibicuí River watershed (ROBAINA et al., 2002; ROBAINA et al., 2015; ROBAINA et al., 2015; RADEMANN et al., 2017; RADEMANN et al., 2018; CABRAL et al., 2020). However, a detailed mapping of erosive features encompassing the entire Santa Maria River Watershed (BHRSM) has not yet been developed, justifying this research. This basin is spatially located over three geomorphological compartments of the state of Rio Grande do Sul (IBGE 1986) and presents a good representation of the current situation of the dynamic transformation of

occupation in which the Pampa Biome is inserted, which is known for the use of native fields with grasses used for cattle pasturing, and which has currently been transformed into crops for agricultural production (Ghersa et al., 2002; Viglizzo et al., 2011; Mengue et al, 2020), which may in the future represent an intensification of surface features. Given the presented, the objectives of this study are: (i) to make an inventory of the ELFs for the BHRSM using high spatial resolution data from GE images; and (ii) to identify and discuss which environmental factors are controlling and triggering the erosive features.

2. Study Area

Located in the southwest of the state of Rio Grande do Sul, between the geographical coordinates 29°47' to 31°36' South latitude and 54°00' to 55°32' West longitude, the BHRSM comprises an area of 15,740 km² (Figure 1). Six municipalities have part or all of their territories inserted in the BHRSM area, being them: Cacequi, Dom Pedrito, Rosário do Sul, Santana do Livramento, São Gabriel and Lavras do Sul.

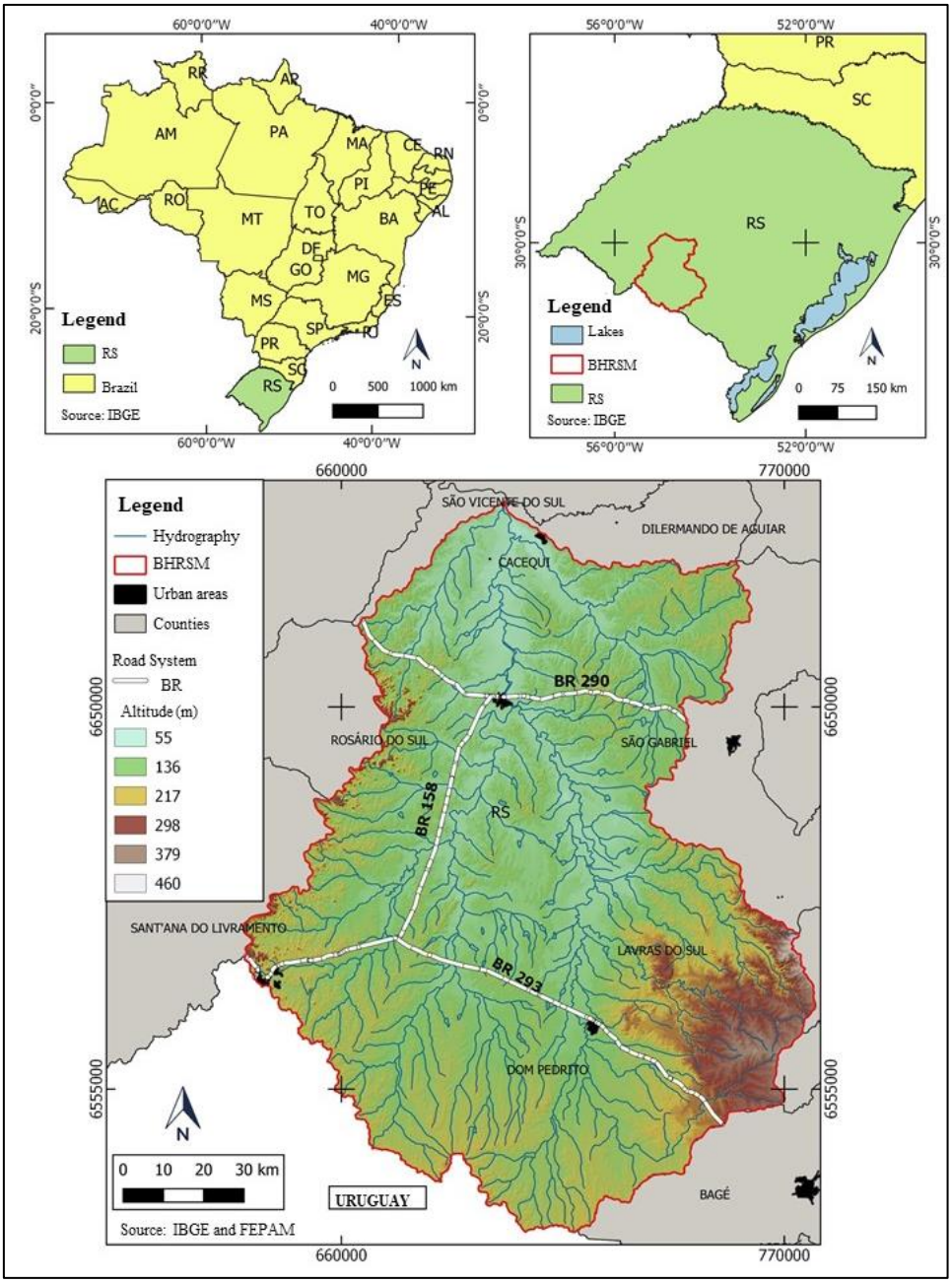

Figure 1. Location of the Santa Maria River watershed, southwest of RS.

The altitudes range from 57 m at its mouth to 455 m in the southeast, in the Cristalino Shield portion. It comprises in its limits three geomorphological provinces, which are: Planalto da Campanha, Depressão Central Gaúcha and Planalto Sul-Riograndense (IBGE 1986). According to Wildner et al (2006), in terms of lithotypes outcropping, the sedimentary sequences of the Paraná Basin stand out. The soils are mostly well developed in terms of profile, being the Argissolos the most common, while the poorly developed soils (Neosolos and Cambissolos) are found in the steep areas and associated with hills (SCOTTI, 2017).

As for land use, field portions predominate, although the area being occupied by crops is increasing, according to Scotti (2017). The climatic typologies found in the BHRSM are: Subtropical I - little humid - and Subtropical II - medium humid - with the average annual temperature ranging from 17 to 20° C and precipitation is around 1,200 - 1,500 mm annually (ROSSATO, 2011).

3. Materials and Methods.

3.1 Data base and spatial information

It was used the Google Satellite image base available in the Geographic Information System QGIS 3.4, through the QuickMap Services plugin. It consists of a repository of time series of high-resolution satellite images (usually around 0.5 m, such as WorldView, Pleiades, GeoEye, etc.) in RGB - visible - view (KARYDAS; PANAGOS, 2020).

The following factors were considered as possible drivers of the LEFs (Table 1): geological substrate; geological fractures and faults; soils and erodibility; hypsometry and slope; slope shape; drainage channels; land use and occupation; and roads.

Table 1. Controlling factors considered, sources, scale, and secondary data obtained.

Data	Source	Scale	Available in	Secondary data obtained
Geological substratum Geological fractures and faults	CPRM	1:750.000	http://geosgb.cprm.gov.br/	Geological fractures and faults
Soil	IBGE/Streck et al. (2008) e Sccoti (2017)	1:250.000	RADAM Project Brazil - IBGE 1986; Rio Grande do Sul Soils	
Soil Erodibility	Bibliography		Mannigel et al. (2002), Silva and Alvares (2005) andLopes et al. (2011)	
Hipsometry Slope Slope curvature profile	SRTM 3 arc second	Spatial resolutionof ~90 m	Earth Explorer (https://earthexplorer.usgs.gov/)	
Drainage system	Continuous RS vector basis	1:50.000	Hasenack andWeber (2010)	
Land use and land cover	Supervised Classification Landsat 8 OLI images	Spatial resolution of 30 meters	Earth Explorer	
Road System	Continuous Vectorial Basis of the RS.	1:50.000	Hasenack and Weber (2010)	

Organized by the authors

The information regarding the lithologies was obtained from the mappings developed by CPRM (WILDNER et al., 2006) and validated in the fieldwork. The soil information was obtained from the mapping proposed by Streck et al (2008) and Sccoti (2017) that split the soils of the BHRSM according to pedogenetic development and hydromorphism into three units. This division was adopted in the present research. The erodibility values (K) were based on the work of Mannigel et al (2002), Silva and Alvares (2005) and Lopes et al (2011) who defined the K values in averages of other 14 authors (Table 2).

Table 2. Erodibility values for the soils identified in the BHRSM.

Soil	Erodibility - Silva and Alvares (2005)	Erodibility - Mannigel et al. (2002) and Lopes et al. (2011)
Platosols	0.0097	
Neosols	0.0351	
Luvisols		0.022
Gleissols	0.0361	
Chernosols	0.0309	
Argissolos	0.0425	

Organized by the authors

The soil erodibility classes were classified by Mannigel et al. (2002), which have defined the range of K (t.h.MJ-1.mm-1) from 0.019 to 0.024 as very low; 0.025 to 0.030 as low; 0.031 to 0.036 as moderate; 0.037 to 0.042 as high and > 0.042 the authors classified as very high. The fieldwork with data survey, descriptions and photographic records, are also used as an adjustment of the cartographic bases for the purpose of adjusting the scales of analysis. The standardization is made necessary for the adequacy of the spatial limits of the classes and association between map layers, which is possible through field investigations.

3.2 Data processing

For the preparation of the slope and hypsometry map, the MDE generated from the SRTM mission (90 m) available at: https://earthexplorer.usgs.gov/ was used. The slope classification followed the assumptions of the Technological Research Institute of São Paulo (IPT), being: 0-2%, 2-5%, 5-15% and more than 15%. To obtain the Plane and Profile, it was used the curvature tool, where the information was generated in raster, and, after the information plane, the reclassification occurred in the four main curvatures: concave-convergent, concave-divergent, convex-convergent and convex-divergent.

Land use was obtained through a supervised classification of LandSat 8 OLI images (Orbit/Point: 223/081 and 223/082), with satellite/sensor system passage on 03/11/2021. The SCP plugin of QGIS 3.10 was used and the statistical method of classification was maximum likelihood. The definition of the classes occurred based on the field work in: Water, Crops, Field, Forest, Forestry and Recent deposits.

3.3 LEF identification and mapping process

As linear erosive features, it is understood the grooves, ravines and gullies, which denote the action of regressive erosion, in the process of wearing away and sculpting the landforms. The term LEF has been used in geomorphological studies, as is the case of the work developed by Yan et al (2008), Zanatta et al. (2015), and Mathias et al. (2020).

The process of identifying linear erosive features was manually performed, through visual interpretation, considering aspects of shapes, tones, textures, and shadows, according to the method adopted by other authors (OLIVEIRA et al., 2013; BOARDMAN, 2016; KNIERIN et al 2018; KARYDAS; PANAGOS, 2020). For the features along the same stream, but interrupted even if by a few meters, these were digitized as separate vectors, according to the methodology of Karydas and Panagos (2020). Finally, a vertex was generated on the mapped lines, corresponding to the head of the first-order channels to correlate with the variables considered in item 3.1 The LEF lines were only considered for the determination of the orientation of the features.

3.4 Mapping accuracy evaluation and fieldwork

It was conducted three field works in order to identify the LEFs: April 20, 2020, August 04, 2020, and April 24, 2021. With the aid of GPS and camera, 55 LEF points were recorded to increase the accuracy of the mapping. Drones were used to validate the analyses by identifying and characterizing the features and illustrating them in the article, but they were not used during the LEF mapping process. It is noteworthy that the points collected are located in the municipalities of Rosário do Sul and Cacequi, along the BR 158, BR 290, RS 640 highways and secondary roads. A calculation was made of the area covered by clouds and shadows, in the database of Google Earth images, and that, therefore, represent areas that cannot be mapped.

3.5 Statistical processing and analysis of the results

In order to generate the circular direction histogram of the LEFs, the "Azimuth" tool, available in the field calculator of the attribute table, was used. Then, this information was inserted into the Line direction histogram plugin to generate the histogram in QGIS 3.4. From the drainage headwaters location file, a LEF concentration map was generated using the "heat map (Kernel density estimate)" tool of QGIS 3.4, with a radius of 6000 map units and quadratic mathematical function.

For the correlation between the data the following steps were created:

To associate the LEF headlands with the parameters of roads and drainages, the "Euclidean distance" tool of ArcGIS was used. The tool has generated a raster file of distances in relation to roads and another file of distance in relation to drainage channels.

As for the data analysis, it is highlighted that the vertices of the first-order drainage headlands with LEF were combined with all the parameters using the "extract value to point" tool of ArcGIS. The tool provided the exact altitude value, slope percentage, distances from roads and drainages, soil type, land use type, slope type and the Geological Formation for each of the LEF headlands.

To correlate the presence of LEFs in the different variable classes of geological substratum, soils, inclination, slope types and land uses and the total percentage occupied in relation to the area of the BHRSM, a frequency ratio (Fr) calculation was applied. The equation adapted from Bonham-Carter (1994) is:

$$Fr = \frac{Fi}{F} / \frac{Ai}{A} \quad (1)$$

Where Ai represents the area occupied by the class of the physical variable "i" within the total area of the BHRSM (A); Fi represents the area of LEF in the physical variable "i", considering the total area of LEF (F).

The values of the frequency ratio (Fr) represent the level of correlation between the LEF and the variable under analysis (geological substratum, soils, inclination, slope types and land uses). Thus, for frequency ratio values greater than 1 (one), the correlation is considered high, while values less than 1 (one) indicates a low correlation (ESPER ANGUIERI, 2013.)

4. Results and discussions

4.1 General characterization of mapped features and mapping

Approximately 5,751 km of mapped linear erosion and 15,090 first-order drainage headwaters were mapped. The mapping process began with a fieldwork for the identification of erosive features. Based on the registered points, it was necessary to understand how these features behaved in terms of tonality and texture elements on satellite images, fundamental criteria for aiding visual interpretation. It is interesting to note that areas of sediment loss with higher reflectance (Figure 2 C) and differentiated texture on the image (Figure 2 D) were more easily identified. The presence of vegetation was also used to aid in the interpretation, since it causes a difference in texture and tonality (Figure 2 A and B). After the mapping performed in the GIS, it was necessary to return to the field to check and validate the process. Only after this step it was possible to extrapolate the mapping for the entire BHRSM. The whole process of surveying the LEFs took about a year.

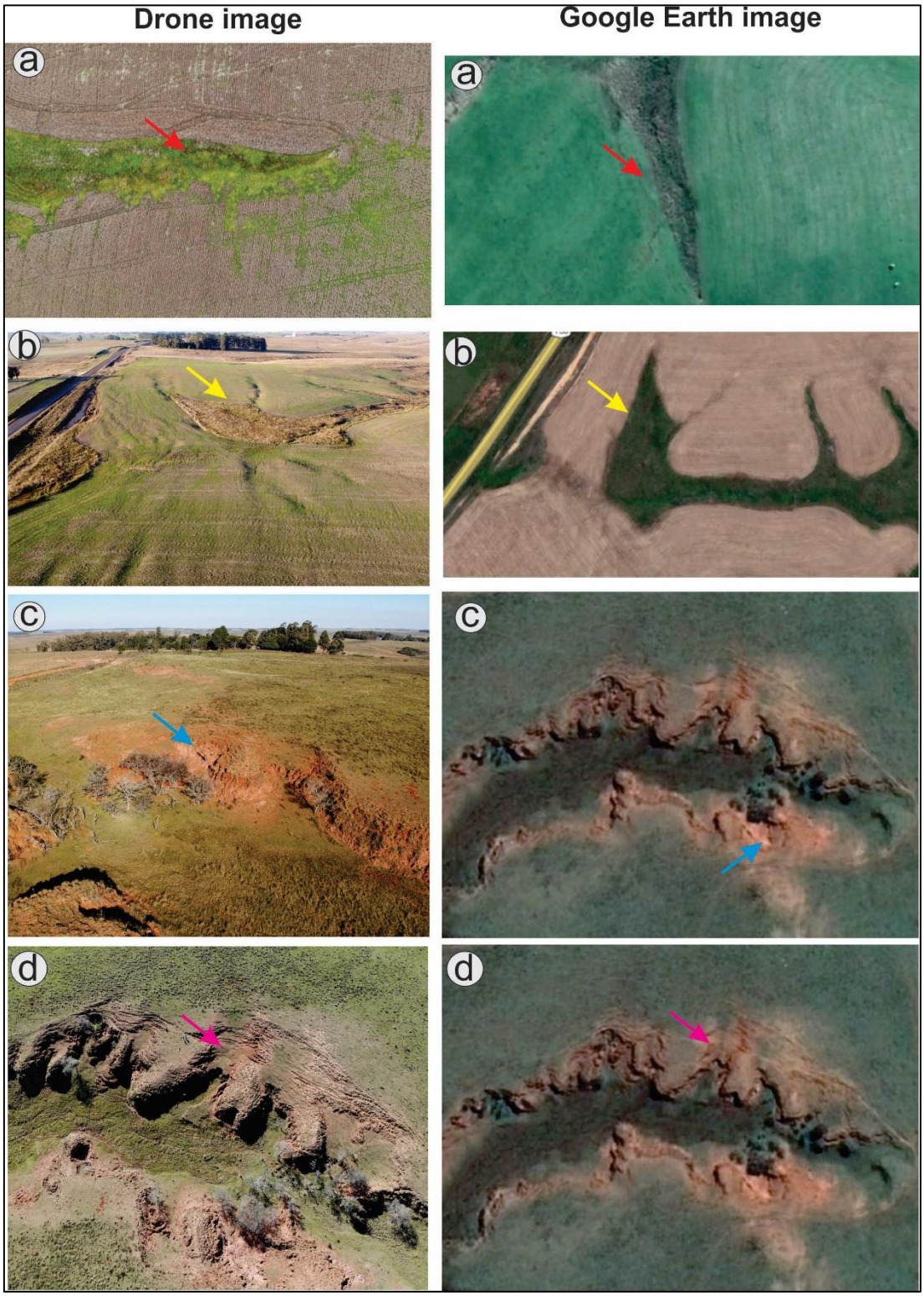

Figure 2. A and B - Showing a gully with vegetation of different color; C - Active gully with the presence of material with high reflectance; D - Degrees of subsidence giving different texture to the portion of the gully. These images have been acquired with the Mavic Air Pro and Mini Mavic drones.

As for the accuracy of the mapping, the calculation of the gaps by clouds and shadows was performed, indicating that 19 km² of area were not available on the Google Earth base, which corresponds to 0.11% of the total study area. It is worth mentioning that the mapping was performed by only one researcher, which contributes to the minimization of errors in image interpretation and subsequent LEF vectorization.

4.2 Determinant factors for the occurrence of linear erosive factores

For the organization of the results and development of the discussions, it was first presented the physical factors that characterize the BHRSM, and then aspects related to the anthropic issue.

4.2.1 Geological substrate

The lithologies that constitute the substratum of the BHRSM are represented by rocks of the Crystalline Massif (Maçico cristalino) and by sequences of sedimentary and volcanic rocks of the Paraná Basin, besides the quaternary sediments (WILDNER et al., 2006). The crystalline Massif occurs in a small portion, to the SE of the BHRSM (Figure 3). The values of Fr are relatively low in this portion, and the highest values were found in areas with occurrence of the Dom Pedrito Granite with FR of 0.408 and volcanics of the Hilario Formation with FR of 0.327.

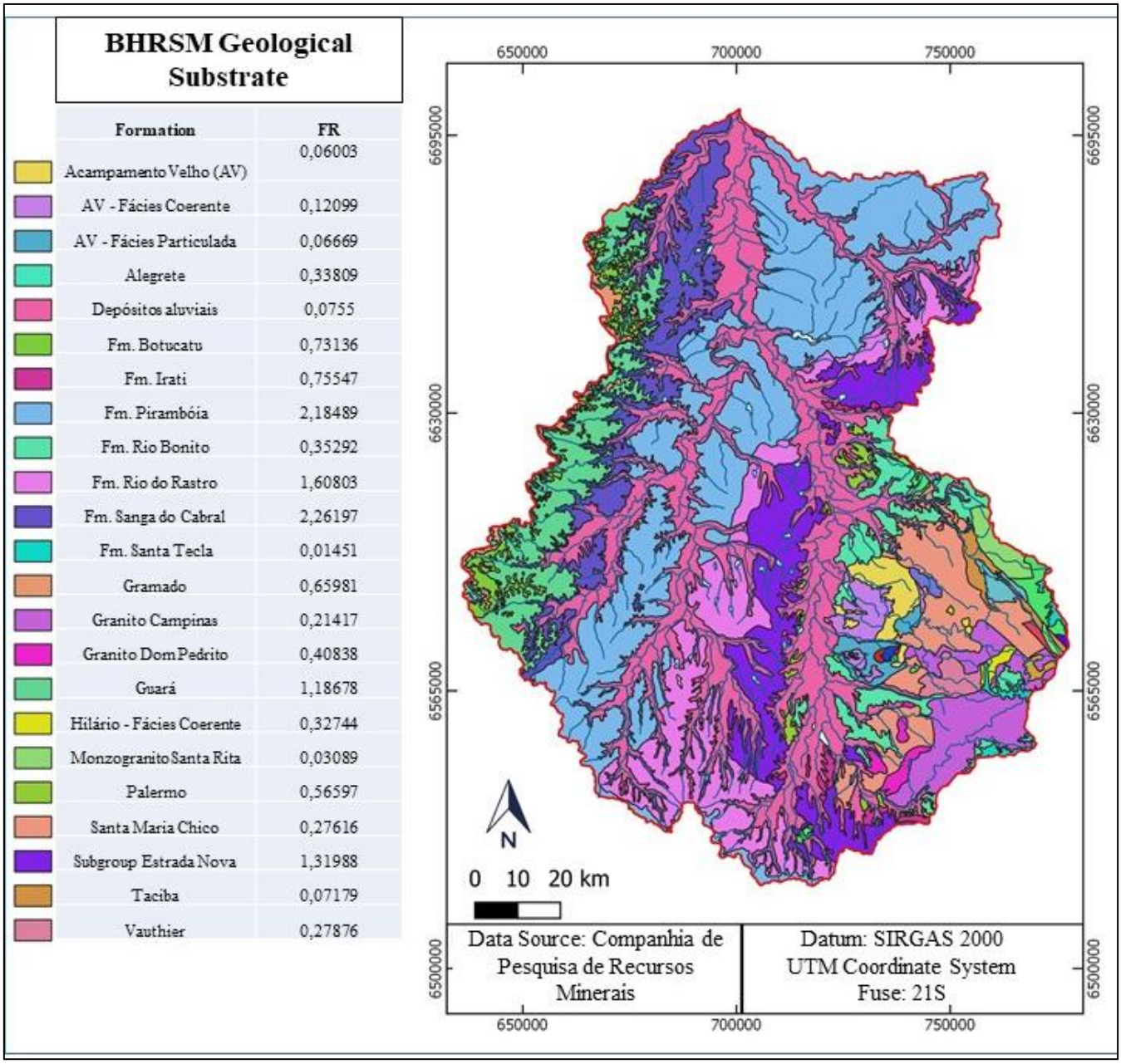

Figure 3. Geological map and respective frequencies of LEF found.

The sedimentary rock sequences from the Paraná Basin occur in the south-central part of the basin. The Rio Bonito Formation presents values of Fr = 0.35, while the Estrada Nova Subgroup, with a Fr value of 1.32, is followed

by sandstones and mudstones, distributed along lateral bands of the Rio do Rastro Formation with Fr = 1.60. These outcrops give way, in western direction, to a thick fluvio-eolian succession. These sequences stand out for the highest Fr values found, being 2.26 for the rocks of the Sanga do Cabral Formation and 2.18 for the rocks of the Pirambóia Formation. It is widely documented by other authors that these two lithologies are more subject to erosion as they are friable rocks (ROBAINA et al., 2010; ROBAINA et al., 2015, RADEMANN et al., 2017; RADEMANN et al., 2018).

Outcropping in the west of the basin (Figure 3) are rocks of the Guará Formation, with Fr = 1.18. In 2015, Robaina et al. (2015) have pointed out that these sandstones demarcate a portion of exposure of sandy, friable materials resulting from aqueous and aeolian erosion. Associated with the Serra do Caverá, which forms the basin divider at the western boundary, there are basalt and basaltic andesite spills that are associated with sandstones of the eolic system of the Botucatu Formation. The volcanic rocks belong to the Alegrete facies, with Fr = 0.338, and the Gramado facies, with Fr = 0.660.

4.2.2 Geological fractures and faults

Analyzing the context of lineaments in the region, Zalán et al. (1990) have pointed out the NW-SE and NE-SO directions as representative of fault and fracture areas for the Paraná River basin and Robaina et al (2002) emphasized that the direction of the gullies in Cacequi (RS) follows tectonic reactivations linked to the development of the mentioned hydrographic basin: "fractures resulting from the NE - SO and NW - SE direction, form a mesh separating blocks on the erosion surfaces" (ROBAINA et al., 2002. p.119). On the other hand, Cabral et al (2020) point the E-O and NE directions as the predominant ones for gullies in Cacequi (RS). In this view, Robaina and Trentin (2019) point out that for the entire Ibicuí watershed there is also strong structural control in the LEFs, with predominant directions of N45(+/-15) E, northeast and N(45+/- 15)W and northwest. In view of this, it is highlighted that the LEFs of the BHRSM develop in areas controlled by Paraná Basin faults, and the gullies end up developing by remontant erosion, following precisely the areas of structural weakness.

Regarding the structural lineaments, the predominant trend of the features is NW-SE or SE-NO (Figure 4). Of all the mapped LEF that correspond to 16,343 vectors, 4,876 have the mentioned directions, that is, approximately 37%. It also stands out that the greatest lengths of LEF are encompassed in this mentioned direction, presuming that the flows concentrated in these planes of weakness provide ease in the incision and formation of gullies and ravines, as well as the greatest development and length as well. The NE-SO direction occurs in approximately 29% of the LEFs, the N-S direction is in about 17% of the LEFs, and L-O in approximately 15% of the LEFs.

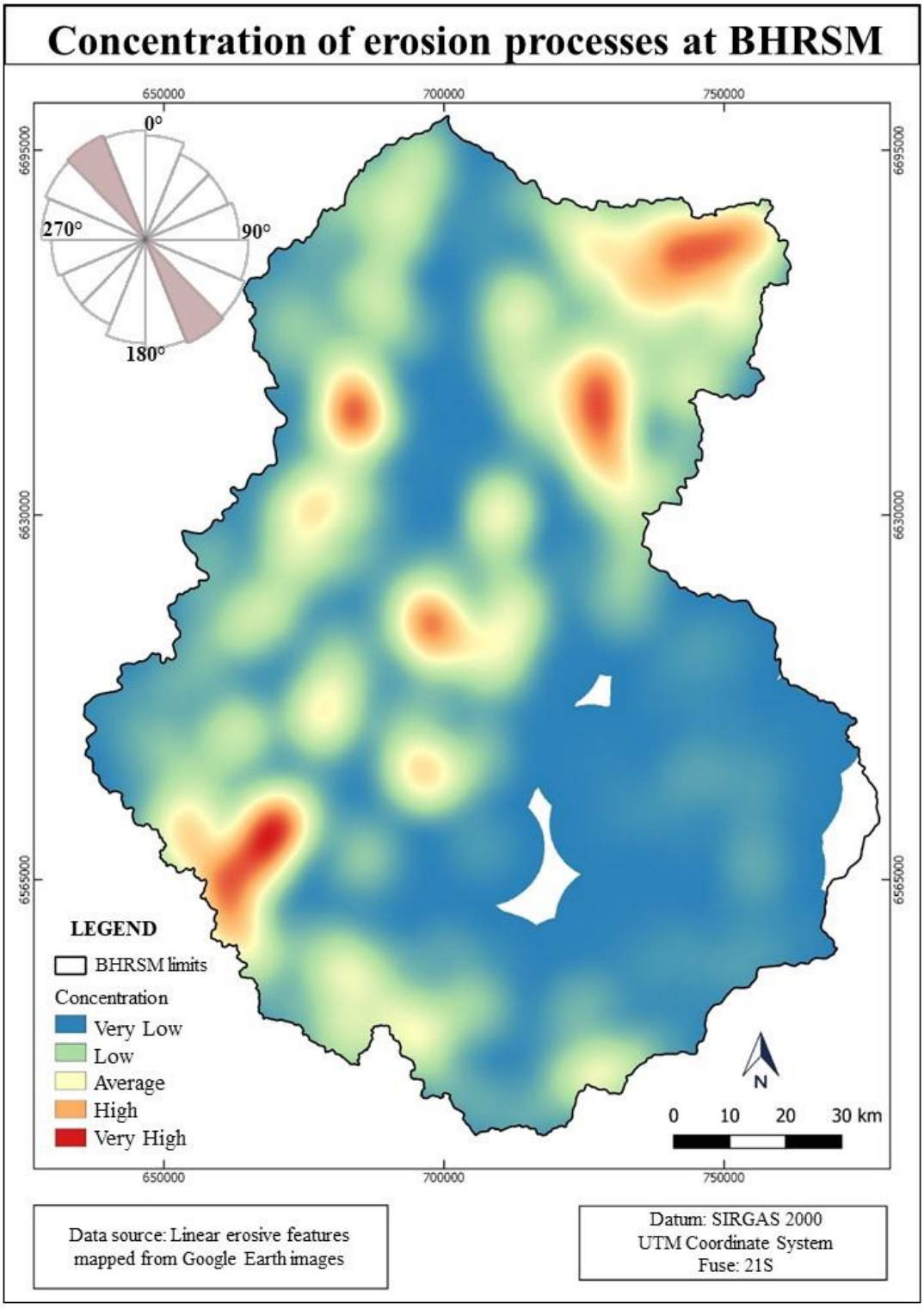

Figure 4. Concentration of erosive processes in the BHRSM, with emphasis on the portion of sedimentary rocks. The direction of the LEFs (NO-SE or SE-NO) correspond to faults and fractures of the Paraná basin.

4.2.3 Soils and erodibility

Considering the first classification level, the soils of the BHRSM are represented by Gleissols, Planosols and Chernosols, Litholic Neosols, Fluvic Neosols, Argissols and Luvissolos. The Neosols present the lowest values of Fr, with the litholic Neosols having a Fr value of 0.17 and the Fluvic Neosols not presenting LEF, dispensing with Fr values.

For soils with hydromorphism, the Planossolos have a correlation value of Fr=0.13, since they are of low erodibility. The Gleissols, despite having moderate erodibility (0.036 t.h.MJ-1.mm-1) according to the Mannigel et al. (2002) classification, had a low Fr of 0.02.

The Chernosols, which were characterized by the organic matter content in the superficial horizon, had a high correlation with linear erosion processes, with Fr value of 1.44. This correlation may be explained by the fact that they are spring areas of the BHRSM, which can be associated with the relief energy and incisive power of hydric fluxes in areas of higher slope (discussed in section 4.2.4). It is also noteworthy that the Chernosols fit in the high erodibility class.

The Argissolos are well-developed soils with a B textural horizon and are considered to exhibit high erodibility, according to the classification of Mannigel et al. (2002), and presented a Fr of 1.53. The Luvissolos, in their turn, which are characterized by textural B and high activity clays, present a significant relation with the linear erosive processes in the basin, having a Fr of 1.25.4.2.4 Hypsometry and Slope.

The predominance of LEFs occurs between the altitudes of 150 to 159 m, which corresponds to 2,536 drainage basin headwaters. In the 160-169 m class, 2,444 drainage headwaters were mapped and in the 140-149 m class, 2,118 drainage headwaters were identified (Figure 5 A). The classes above 220 m together possess less than 2.5% of the LEF and, even though in these areas the slopes are steeper, there is more emphasis on other forms of material transport. Compared to other studies, such as in the municipality of Unistalda (RS), in the work of Knierin et al. (2018), it was also observed the erosion pattern in altitudes lower than 200 m. The highest portions (>200 m) of the BHRSM correspond to the Cristalino Shield and the Serra do Caverá, in areas of litholic neosols and rocky outcrops, therefore, areas with less possibility of LEF development.

As for slope, most of the drainage headlands with LEF are in the classes between 2-5% and 5-15%, respectively with 6,685 and 6,620 features (Figure 5 B). However, when is calculated the frequency value is, there are more LEF for the 5-15% class, with Fr=2.60. For Unistalda (RS), Knierin et al. (2018) observed the erosive features developing mainly in the 5-15% class and for Cacequi (RS), Rademann et al. (2018) also verified the same result. Trentin and Robaina (2015) emphasize that slopes greater than 5%, in general, promote the development of erosion.

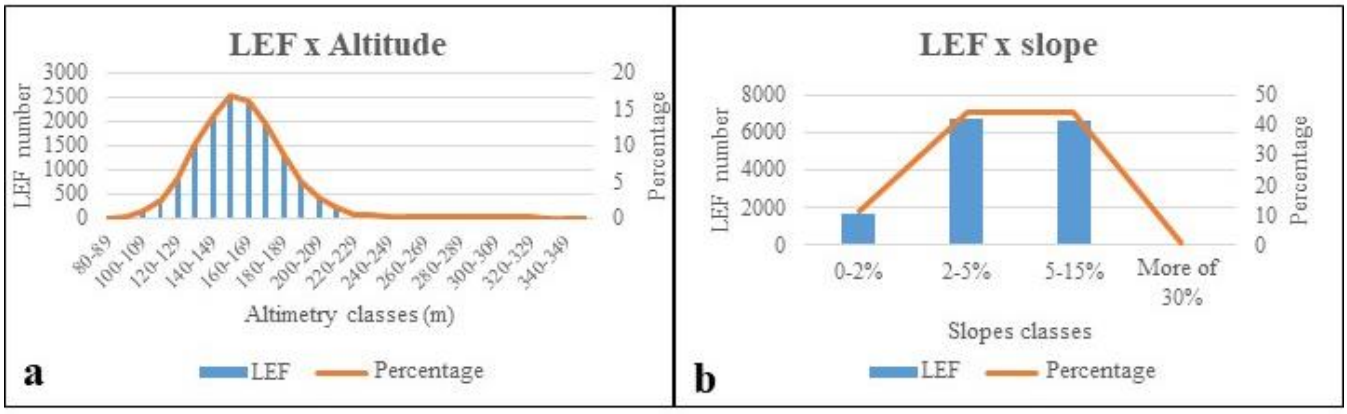

Figure 5. Frequency observed of drainage headlands with LEF, according to hypsometric class (a), and slope (b)

4.2.5 BHRSM curvature profile

The prevalence of LEF headwaters is observed in the concave-convergent hillslopes with Fr=1.22 and convex-convergent with Fr=1.34, observing a strong control established by the horizontal curvature. The convergent hillslopes are characterized by concentrating the flows of matter and energy and, consequently, triggering erosive processes in the springs (Figure 6). The results are in line with other studies, such as the one conducted by Knierin et al. (2018), which have also identified in Unistalda/RS the predominance of erosive processes in concave and convergent plane profiles; and Cabral et al. (2020) have highlighted that the erosive features of Cacequi/RS develop on slopes with convex bases, at higher slopes and small ramp lengths, favoring the increase in runoff velocity.

It is noteworthy that for the BHRSM only 23% of the slopes are of the convergent type, with a predominance of the divergent profile slope. There is a predominance of concave-divergent slopes occupying about 76% of the area, with a Fr=0,92 for the presence of LEF. Although this is not a profile that favors the concentration of surface runoff,

it is important to mention that other parameters can influence this runoff, such as slope, soils and geology, as well as anthropic interventions related to land use or road implantation (presented in the next sections). The schemes arranged on the left (Figure 6) demonstrate the incision of the LEFs associated with the drainage network (the last one is presented in more detail in section 4.2.6).

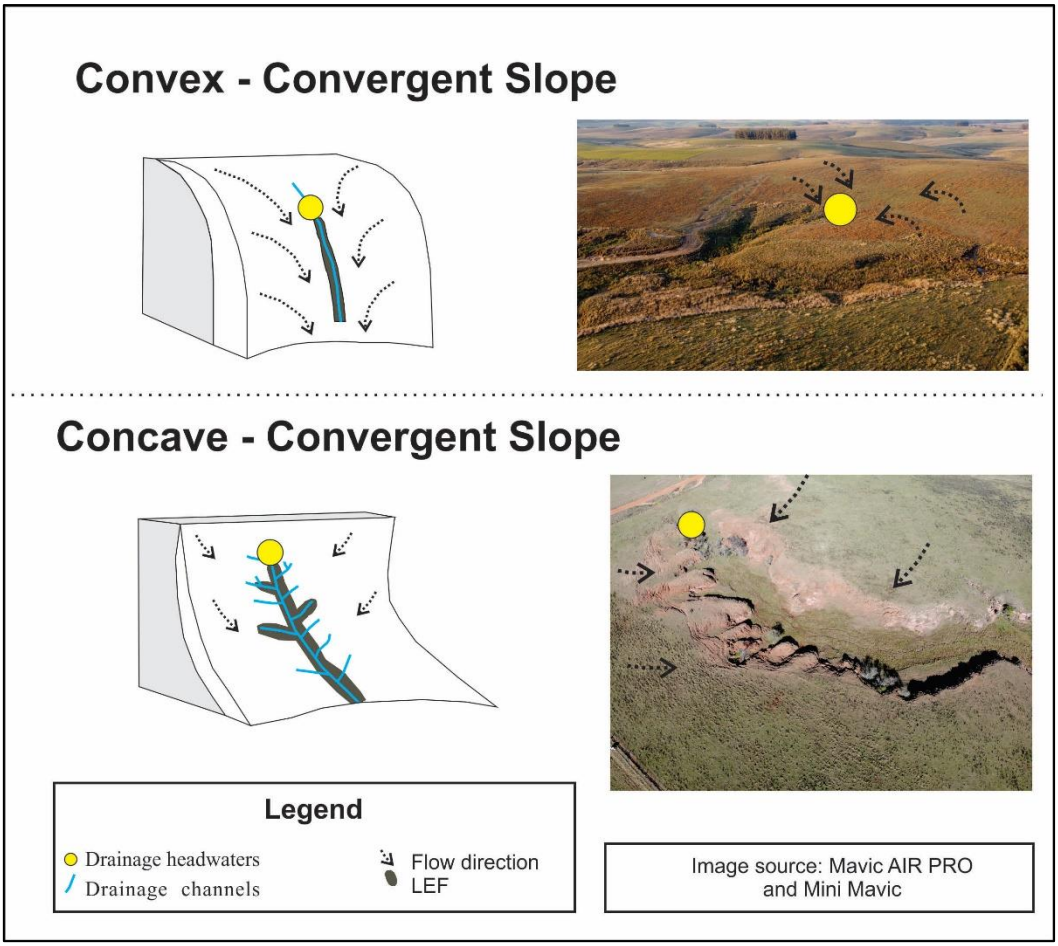

Figure 6. Diagram of the shapes of the slopes with the presence of LEF.

4.2.6 Drainage Channels

About 25% of the LEFs are located in drainage headwaters, associated with a range of 0-100 m from the BHRSM channels (Figure 7 A); on the other hand, 20% are located at a distance between 101-200 m from these channels and 25% were mapped between 201-300 m; finally, 15% are located between 401-500 m, and only 15% of the LEFs are located in the range between 501-700 m from the headwaters. After the 701 m distance line from the drainage channels, there are no nearby LEFs, which demonstrates the strong association of these features with the drainage system. This association has contributed to expand connectivity in the landscape, that is, the relationship between erosion features and watercourses, thus increasing the potential for sediment transfer to the watercourses. These are areas of concentrated flow in portions of friable soils, which in precipitation events carry a large amount of sediments to the perennial drainage channels, causing silting and changes in the fluvial morphology. Associated with the morphological and morphometric conditions, we a system of fractures was presented (section 3.2.2), where the drainage network was installed, as the talweg deepens and advances according to the remounting erosion. This process is natural in the BHRSM and is associated with its morphodynamics, and can be accelerated by anthropic actions.

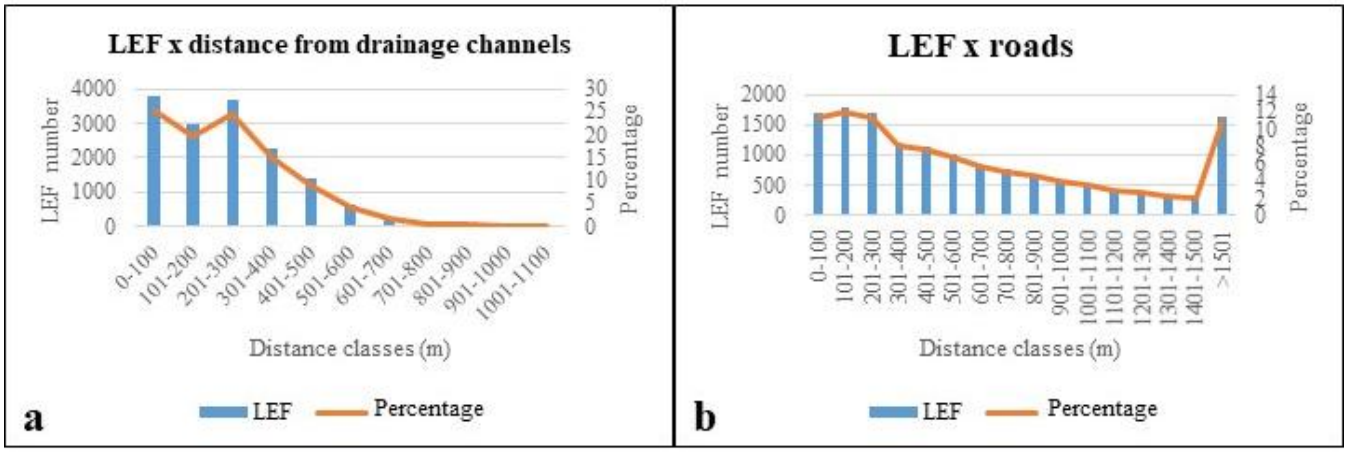

Figure 7. Observed frequency of drainage headwaters with LEF, according to distance from drainage channels (a) and distance from roads (b).

In the aforementioned study on linear erosive features, which was conducted by Knierin et al. (2018), the occurrence of erosive processes associated with the drainage network and those associated with the base of hills, hillsides and/or cornices was highlighted. It has been observed that LEFs in the BHRSM are associated with first-order channels (Figure 8 B and 8 C; Figure 9 C), for the most part. The association of LEF with hills and hillsides occurs only in the southwestern portions (Figure 8 A) of the BHRSM, in the Serra do Caverá.

Figure 8. LEF developing near a hillside (a); near a reservoir (b) and in intermittent drainage channels (c).

4.2.7 Use and land occupation

The highest value of Fr has been found for the field portions, being equal to 1.37, which has also been noticed in field work in the BHRSM, when observing the role of erosion caused by animals, such as cattle. It is common to observe that the paths created by cattle, by causing soil compaction, act as channels to facilitate surface runoff (Figure 9 D and E). In some of the margins of the gullies it is possible to see the destabilization of these portions, due to the passage of cattle, promoting the development of abatement steps (Figure 9 F).

For the areas of temporary crops a Fr=0.72 was obtained, representing a lower correlation. However, it is highlighted that Sccoti et al. (2015) and Sccoti (2017) have already addressed that it is possible to verify a transition from field to crop areas. Comparing the 2001 mapping done by Sccoti (2017) with the one performed in this research in 2021, the areas with crops doubled - they used to occupy 13% of the BHRSM and currently this number corresponds to 26%; while the field areas represented 67% and in 2021, were reduced to 55% of the BHRSM. On the field, it was observed that some properties did not use the no-till farming management technique, promoting the transport of sediments by laminar and linear erosion. It is necessary to adopt no-till farming in all the properties, avoiding the period of soil exposure from temporary crops, since the natural characteristics of the soil already imply fragility to erosion. For the forestry category the Fr registered was 0.06 and for forests it was 0.14, highlighting that these are types of land use that occupy small areas of the BHRSM (305 km² and 943 km², respectively).

4.2.8 Roads

Over 56% of the LEF headlands were found in the vicinity of roads (0-600 m). Specifically, 23% of the headlands were found in the class between 0-200 m from roads (Figure 7 B); 19% between 201-400 m away from roads and 14% of the headlands in a range between 401-600 m. Between 600-1000 m, about 19% of the headlands are found with LEF. Above 1,000 m, approximately 25% of the LEF are present in the headlands, demonstrating the little influence of roads for the development of linear erosion in these portions, therefore other environmental factors prevail as determinants (for example slope, hypsometry, slope curvature and soils).

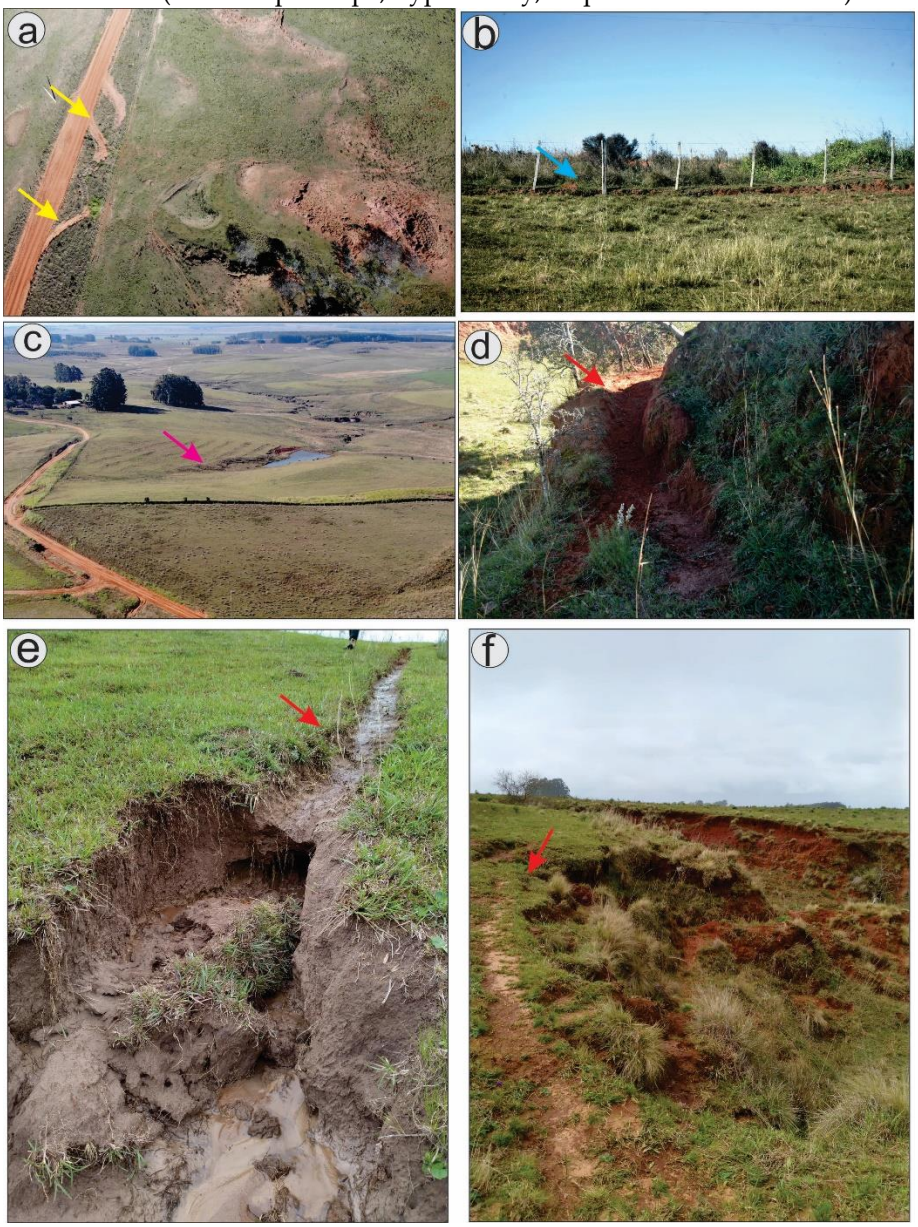

Figure 9. A - structure built for rainfall-runoff on a secondary road, just upstream of a gully; B - erosion developing parallel to a cattle fence; C - LEF connected to a water tank, in a first-order channel; D and E - LEF developing in a field area (the red arrow indicates the path taken by cattle, soil compaction and concentration of surface runoff); F - Path created by cattle on the margin of a gully, contributing to the reduction of a step. Images A and C were acquired with Mavic Air Pro drone.

On the field, it was possible to observe that at some points of the highways and secondary roads, there are headwaters with LEF, resulting from the concentration of rainwater flow in gutters or runoff channels (Figure 9 A), while it is also observed that remontant erosion itself occurs in this regression of the valley headwaters, up to the point of the road. Therefore, it can affect the residents' traffic, as observed in the municipality of Cacequi (RS),

where a "caution" demarcation was found on the road due to the large gully formed on the marginal portion (29°58'37.21 "S; 54°37'2.48 "W).

Moreover, as exposed by Poesen (1993) and Augustin and Aranha (2006) other linear elements may have an influence on the development of concentrated flows, such as plot boundaries, fences (Figure 9 B), and cattle trails (Figure 9 D, E and F), especially since the LEFs develop predominantly in field areas, according to the previous section.

5. Conclusions

Regarding the method, it is highlighted that despite being extremely time-consuming, taking months between the vectorization process and field evaluation, there were significant results due to the spatial scale of detail achieved. Therefore, it is emphasized that interpretation keys based on texture, tonality, reflectance, and position in the landscape are fundamental to assure the accuracy of the mapping, thus allying field observations to geoprocessing.

It is noteworthy that the erosive processes in the BHRSM are associated with the types of rocks present in the area, with little consolidated sandy substrate, configuring a natural process, as shown in the section on geology and soils. Besides the lithostructural conditioning, through the development of LEF in portions of geological fractures, it has been observed that there is an association with the land relief energy by promoting the increase of water runoff velocity over friable sandstones. The relief energy for the incision of water flows is preponderant when discussing the relationship with the soil, since the force of water percolation ends up causing soil dismantling processes, especially in the mid-slope portions. The portions with higher Fr are related to slopes between 5-15% and below 200 m altitude.

Despite being a natural phenomenon, human presence accelerates the erosive processes. The presence of cattle and the construction of fences have been shown to be determining features for the occurrence of linear erosion processes in portions of the land use and occupation category called fields, and roads concentrate more than 50% of the LEF in their immediate vicinity (0-600 m). Furthermore, agricultural activities can cause changes in the period of seasonal soil cover and changes in nutrient and organic matter content, due to the intensification of the transition from field use to soybean farming. It was verified that the area occupied by crops has doubled in the period of 20 years, when compared to the research of Sccoti (2017) - configuring new conditions of use and occupation for the BHRSM, demanding monitoring for the coming years in order to follow the adaptation of hydrosedimentological systems to this new scenario.

As for future works, it is suggested that investigations focused on the determination of the erodibility factor of soils for the BHRSM and on obtaining geomorphometric data at a larger scale of detail take place. On the other hand, it is considered a valuable scientific contribution, the continuity of this research with regard to the realization of the classification of only the gullies for the entire BHRSM.

Author's contributions: Carina Petsch: Conceptualization, Formal Analysis, Acquisition of Funding, Research, Methodology, Resources, Validation, Writing; Anderson Augusto Volpato Sccoti: Conceptualization, Formal Analysis, Research, Methodology, Validation, Writing; Luís Eduardo de Souza Robaina: Formal Analysis, Research, Methodology, Writing; Romario Trentin: Formal Analysis, Research, Methodology, Writing

Funding: The authors thanks the Fundação de Amparo à Pesquisa do Estado do Rio Grande do Sul (process 19/2551-0001234-9).

Conflict of Interest: The authors declare no conflict of interest.

Referências

1. AMIRI, H.; POURGHASEMI, H. R.; GHANBARIAN, G. A.; AFZALI, S. F. Assessment of the importance of gully erosion effective factors using Boruta algorithm and its spatial modeling and mapping using three machine learning algorithms. **Geoderma**, v. 340, p. 55-69, 2019. DOI: 10.1016/J.GEODERMA.2018.12.042
2. AGHARAZI, H; DAVOUDIRAD, A. A; KHOSROBAGI, S., SHADFAR, S.; NIKCHAH, S.; NAJIM, A. Gully erosion Sufficiency mapping at Robatturk Watershed (Iran) using an artificial neural network model. **International Journal of Computer Science and Network Security**, v. 17, n. 4, p. 14, 2017. DOI: 10.1080/19475705.2020.1753824

3. AGNESI, V.; ANGILERI, S.; CAPPADONIA, C.; CONOSCENTI, C.; ROTIGLIANO, E. Multi-parametric GIS analysis to assess gully erosion susceptibility: a test in southern Sicily, Italy. **Landforms Analysis**, v. 7, p. 15–20. 2011.
4. BATISTA, D. C. L.; VIEIRA, A. F. S. G.; MARINHO, R. R. Utilização do "Google Earth Pro" no mapeamento de voçorocas na área urbana de Manaus (AM), Brasil. **Geosaberes**, v. 10, n. 20, p. 1-12, 2018. DOI: 10.26895/geosaberes.v10i20.689
5. BOUCHNAK, H.; FELFOUL, M.S.; BOUSSEMA, M. R.; SNANE, M. H. Slope and rainfall effects on the volume of sediment yield by gully erosion in the Souar lithologic formation (Tunisia), **CATENA**, v. 78, n. 2, p. 170-177, 2009. DOI: 10.1016/j.catena.2009.04.003.
6. BONHAM CARTER, G. F. **Geographic Information Systems for Geoscientists: Modelling with GIS**. Oxford: Pergamon, 1994, 391 p.
7. BOARDMAN, J. The value of Google Earth™ for erosion mapping, **CATENA**, v. 143, p. 123-127, 2016. DOI: 10.1016/j.catena.2016.03.031.
8. BRAGA, L.; FERREIRA, R. S.; UAGODA, R. Mapeamento de feições erosivas e análise dos fatores controladores da erosão na bacia hidrográfica do Ribeirão Contagem-DF. **Espaço & Geografia,** v. 20, n. 1, 2017.
9. CABRAL, T. L.; NUMMER, A. V.; BATEIRA, C. V. de M. Indicadores morfométricos como suporte para a classificação de voçorocas em sub-bacias hidrográficas no município de Cacequi, RS**. Revista Brasileira Geomorfologia**, v.21, n.1, p.139-154, 2020. DOI: 10.20502/rbg.v21i1.1670
10. CASTRO, U. N.; NEVES, S. R. A.; SILVA, L. F. T. C.; MENDES, S. P. M.; GUERRA, A. J. T. Mapeamento de feições erosivas e cicatrizes de escorregamento por unidades de relevo na sub-bacia do rio Sana (Macaé – RJ). **Revista de Geografia.** v. especial VIII SINAGEO, n. 3, 2010. DOI: 10.51359/2238-6211.2010.228896
11. CONFORTI, M.; AUCELLI, P.P.C.; ROBUSTELLI, G; SCARCIGLIA, F. Geomorphology and GIS analysis for mapping gully erosion susceptibility in the Turbolo stream catchment (Northern Calabria, Italy). **Natural Hazards,** v. 56, p. 881–898, 2011. DOI: https://doi.org/10.1007/s11069-010-9598-2
12. CUI, P.; LIN, Y.; CHEN, C. Destruction of vegetation due to geo-hazards and its environmental impacts in the Wenchuan earthquake areas. **Ecological Engineering,** v. 44, p. 61–69, 2012. DOI: 10.1016/j.ecoleng.2012.03.012
13. DESPRATS, J.; RACLOT, D.; ROUSSEAU, M..; CERDAN, O.; GARCIN, M.; LE BISSONNAIS, Y.; BEN SLIMANE, A.; FOUCHE, J.; MONFORT-CLIMENT, D. Mapping linear erosion features using high and very high resolution satellite imagery. **Land Degradation & Development,** v. 24, p. 22-32, 2013: DOI: 10.1002/ldr.1094
14. EL MAAOUI M.A.; FELFOUL M. S.; BOUSSEMA M.R; SNANE, M.H. Sediment yield from irregularly shaped gullies located on the Fortuna lithologic formation in semi-arid area of Tunisia. **CATENA**, v. 93, p. 97–104, 2012. DOI: 10.1016/j.catena.2012.02.004
15. ESPER ANGLIERI, M. Y. Debris flow susceptibility mapping in a portion of the Andes and Preandes of San Juan, Argentina using frequency ratio and logistic regression models. **Earth Sciences Research Journal**, v. 17, n. 2, p. 159-167, 2013.
16. Esri Inc. ArcMap (versão 10.4.1). Redlands, Estados Unidos, 2016.
17. GHERSA C.M., FERRARO D.O., OMACINI M., MARTÍNEZ-GHERSA M.A., PERELMAN S., SATORRE E.H., SORIANO A. Farm and landscape level variables as indicators of sustainable land-use in the Argentine Inland-Pampa. **Agriculture, Ecosystems and Environment**, v. 93, n. 44199, p. 279-293. 2002. DOI: 10.1016/S0167-8809(01)00351-6.
18. HASENACK, H.; WEBER, E. **Base Cartográfica Vetorial Contínua do Rio Grande do Sul. Escala 1:50.000**. Porto Alegre: UFRGS, 2010.
19. INSTITUTO BRASILEIRO DE GEOGRAFIA E ESTATÍSTICA (IBGE). Projeto RADAMBRASIL. Levantamento de recursos naturais (Folha SH.22 Porto Alegre e parte das Folhas SH.21 Uruguaiana e SI.22 Lagoa Mirim). 1. ed. Rio de Janeiro: [s.n.], 1986
20. KARYDAS, C.; PANAGOS, P. Towards an Assessment of the Ephemeral Gully Erosion Potential in Greece Using Google Earth. **Water**, v. 12, n. 2, p. 603, 2020. DOI: 10.3390/w12020603
21. KNIERIN, I. da SILVA; TRENTIN, R.; ROBAINA, L. E. de S. Relação dos processos erosivos lineares com os atributos do relevo no município de Unistalda - RS. **GeoUERJ**, n. 32, p. e23397, 2018. DOI: 10.12957/geouerj.2018.23397
22. LIU, K.; DING, H., TANG, G.; NA J.; HUANG, X.; XUE, Z.; YANG, X.; LI, F. Detection of Catchment-Scale Gully-Affected Areas Using Unmanned Aerial Vehicle (UAV) on the Chinese Loess Plateau. **ISPRS International Journal of Geo-Information**. v.5 (12), p. 238, 2016. DOI: 10.3390/ijgi5120238
23. LOPES, F. B. L.; ANDRADE, E, M.; TEIXEIRA, A. S.; CAITANO, R. F.; CHAVES, L. C. G. Uso de geoprocessamento na estimativa da perda de solo em microbacia hidrográfica do semiárido brasileiro. **Revista Agro@mbiente On-line**, v. 5, n. 2, p. 88-96, 2011.

24. LUCÀ, M. CONFORTI, G. ROBUSTELLI. Comparison of GIS-based gullying susceptibility mapping using bivariate and multivariate statistics: Northern Calabria, South Italy. **Geomorphology**, 134 (2011), pp. 297-308. DOI: 10.1016/j.geomorph.2011.07.006
25. MANNIGEL, A. R.; CARVALHO, M. P.; MORETI, D.; MEDEIROS, L. R. Fator erodibilidade e tolerância de perda dos solos do Estado de São Paulo. **Acta Scientiarum Agronomy**, v. 24, n. 5, p. 1335-1340, 2002. DOI: 10.4025/actasciagron.v24i0.2374
26. MATHIAS, D. T.; LUPINACCI, C. M.; NUNES, J. O. R. Identificação dos fluxos de escoamento superficial em área de relevo tecnogênico a partir do uso de modelos hidrológicos em SIG. **Sociedade & Natureza**, v. 32, p. 820-831, 2020. DOI: 10.14393/SN-v32-2020-49431
27. MENÉNDEZ-DUARTE, R.; MARQUÍNEZ, J.; FERNÁNDEZ-MENÉNDEZ, S.; SANTOS R. Incised channels and gully erosion in Northern Iberian Peninsula: Controls and geomorphic setting, **CATENA**, v. 71, n. 2, p. 267-278, 2007, DOI: 10.1016/j.catena.2007.01.002
28. MENGUE, V. P; FREITAS, M. W. D.; SILVA, T. S.; FONTANA, D. C.; SCOTTÁ, F.C. LAND-USE and land-cover change processes in Pampa biome and relation with environmental and socioeconomic data. **Applied Geography**, v. 125, p. 1–12, 2020. DOI: 10.1016/j.apgeog.2020.102342.
29. MONTANARELLA, L. et al; World's soils are under threat. **Soil**, n. 2. 2016. DOI: 10.5194/soil-2-79-2016.
30. OLIVEIRA, B. E. N.; MATRICARDI, E. A. T.; CHAVES, H. M. L.; BIAS, E. S. Identificação dos processos erosivos lineares no Distrito Federal através de fotografias aéreas e geoprocessamento. **Geociências**. v. 32, n. 1, 2013.
31. POESEN, J.; NACHTERGAELE, J.; VERSTRAETEN, G.; VALENTIN C. Gully erosion and environmental change: importance and research needs. **CATENA**, v. 91 p. 91-133,2003. DOI: 10.1016/S0341-8162(02)00143-1
32. QGIS Development Team. QGIS Geographic Information System (versão 3.4). 2021. Disponível em: <http://qgis.osgeo.org>.
33. RADEMANN, L. K.; TRENTIN, R.; ROBAINA, L. E. de S. Relação das variáveis ambientais com os processos erosivos no município de Cacequi, Rio Grande do Sul. **Revista Geoaraguaia**. v. 8 n. 2, 2018.
34. RADEMANN, L. K.; TRENTIN, R.; ROBAINA, L. E. de S. **Relação do substrato litológico com os processos erosivos no município de Cacequi, Rio Grande do Sul.** In: Peres Filho, A.; AMORIM, R. R. (org.). Campinas: UNICAMP - XVII Simpósio Brasileiro de Geografia Física. 2017, p. 6545-6549, DOI: 10.20396/sbgfa.v1i2017.2575
35. RAHMATI, O.; HAGHIZADEH, A.; POURGHASEMI, H.R.; NOORMOHAMADI, F. Gully erosion susceptibility mapping: the role of GIS-based bivariate statistical models and their comparison. **Natural Hazards**, v. 82, p. 1231–1258, 2016. DOI: 10.1007/s11069-016-2239-7
36. RAJESH B.V.; SHRUTHI, N. K.; JETTEN, V.; STEIN, A. Object-based gully system prediction from medium resolution imagery using Random Forests. **Geomorphology**, v. 216, p. 283-294, 2014. DOI: 10.1016/j.geomorph.2014.04.006
37. RAZAVI-TERMEH, S. V.; SADEGHI-NIARAKI, A.; CHOI, S. Gully erosion susceptibility mapping using artificial intelligence and statistical models. **Geomatics, Natural Hazards and Risk**, v. 11:1, p. 821-844, 2020. DOI: 10.1080/19475705.2020.1753824
38. ROBAINA, L. E. de S.; FERNANDES NETO, S.; PAULA, P. M.; PEREIRA, V. P. Processo erosivo acelerado no RS: voçorocamento no município de Cacequi. **GEOGRAFIA**, v. 27, n.2, p. 109-120, 2002.
39. ROBAINA, L.E.S.; TRENTIN, R.; BAZZAN, T.; RECKZIEGEL, E.W.; VERDUM, R.; DE NARDIN, D. Compartimentação geomorfológica da bacia hidrográfica do Ibicuí, Rio Grande do Sul, Brasil: proposta de classificação. **Revista Brasileira de Geomorfologia**, v.11, n.2, p.11-23, 2010. DOI: 10.20502/rbg.v11i2.148
40. ROBAINA, L.E.S.; TRENTIN. Estudo das erosões lineares profundas e o uso do solo na bacia do rio Ibicui/RS. In: BERRETA, M.S.R.; LAURENT, F. (ed.) **Mudanças nos sistemas agrícolas e territórios no Brasil**. 1ª Ed. Porto Alegre - RS: Uergs, Université Le Mans, 2019. p. 178-2005. DOI: 10.21674/9788560231.178-205
41. ROBAINA, L.E.S.; TRENTIN, R.; LAURENT, F; SCCOTI, A. A. V. Zoneamento morfolitológico da bacia hidrográfica do rio ibicuí e sua relação com processos superficiais e o uso do solo. **Revista Brasileira de Geomorfologia**, v. 16, n. 1, p. 63-77, 2015. DOI: 10.20502/rbg.v16i1.630
42. ROSSATO, M. S. **Os climas do Rio Grande do Sul: variabilidade, tendências e tipologia.** Tese (Doutorado em Geografia) Programa de Pós-Graduação em Geografia, Universidade Federal do Rio Grande do Sul, Porto Alegre. 2011. 240p.
43. SARTORI, M., PHILIPPIDIS, G., FERRARI, E., BORRELLI, P., LUGATO, E., MONTANARELLA, L., PANAGOS, P. A linkage between the biophysical and the economic: Assessing the global market impacts of soil erosion. **Land Use Policy,** v. 86, p. 299-312, 2019. DOI: 10.1016/j.landusepol.2019.05.014
44. SCCOTI, A. A. V. **Zoneamento geoambiental da bacia hidrográfica do rio Ibicuí da Armada-RS: potencialidades e suscetibilidade**. (Mestrado em Geografia) Programa de Pós-Graduação em Geografia, Universidade Federal de Santa Maria, Santa Maria. 2015.

45. SCCOTI, A. A. V. **Estudo e zoneamento geoambiental com auxílio de sig na bacia hidrográfica do Rio Santa Maria: sudoeste do Estado do Rio Grande do Sul.** Tese (Doutorado em Geografia) Programa de Pós-Graduação em Geografia, Universidade Federal do Rio Grande do Sul, Porto Alegre. 2017. 153p.
46. SHRUTHI, R.B.B.; KERLE, N.; JETTEN, V.; ABDELLAH, L.; MACHMACH, I. Quantifying temporal changes in gully erosion areas with object oriented analysis, **CATENA**, v. 128, p. 262-277, 2015. DOI: 10.1016/j.catena.2014.01.010
47. SILVA, A. M.; ALVARES, C. A. Levantamento de informações e estruturação de um banco dados sobre a erodibilidade de classes de solos no estado de São Paulo. **Geociências**, v. 24, n. 1, p. 33-41, 2005.
48. SOUZA, N.C.; PITOMBO, C. CUNHA, A.L.; LAROCCA, A.P.C.; ALMEIDA FILHO, G.S. Modelo de classificação de processos erosivos lineares ao longo de ferrovias através de algoritmo de árvore de decisão e geotecnologias. **Boletim de Ciências Geodésicas**, v. 23, n. 1, p.72 - 86, 2017. DOI: 10.1590/S1982-21702017000100005
49. STRECK, E.V.; KÄMPF, N.; DALMOLIN, R. S. D.; KLAMT, E.; NASCIMENTO, P. C.; SCHNEIDER, P.; GIASSON, E.; PINTO, L. F. S. **Solos do Rio Grande do Sul**. Porto Alegre: UFRGS, 2008. 222 p.
50. SVORAY, T. MICHAILOV, E. COHEN, A. ROKAH, L. STURM. A. Predicting gully initiation: comparing data mining techniques, analytical hierarchy processes and the topographic threshold. **Earth Surface Processes and Landforms,** v. 37 (6), p. 607-619. 2012. DOI: 10.1002/esp.2273
51. TRENTIN, R.; ROBAINA, L.E.S.; SILVEIRA, C. T. Compartimentação geomorfométrica da bacia hidrográfica do rio Itú/RS. **Revista Brasileira de Geomorfologia**, v.16, n.2, p.219-237, 2015. DOI: 10.20502/rbg.v16i2.460
52. VALENTIN, C.; POESEN, J.; LI, Y. Gully erosion: Impacts, factors and control. **CATENA**, v. 63, p. 132–153, 2005. DOI: 10.1016/j.catena.2005.06.001
53. VANWALLEGHEM, T.; POESEN, J.; NACHTERGAELE, J.; VERSTRAETEN, G. Characteristics, controlling factors and importance of deep gullies under cropland on loess-derived soils. **Geomorphology**, v. 69, p. 76-91, 2005. DOI: 10.1016/j.geomorph.2004.12.003
54. VIGLIZZO, E. F.; FRANK, F. C.; CARREÑO, L.V.; JOBBÁGY, E. G.; PEREYRA, H.; CLATT, J.; PINCÉN D.; RICARD M. F. Ecological and environmental footprint of 50 years of agricultural expansion in Argentina. **Global Change Biology**, v. 17, n. 2, p. 959-973. 2011. DOI: 10.1111/j.1365-2486.2010.02293.
55. VRIELING, A. Satellite remote sensing for water erosion assessment: A review. **CATENA**, v. 65, n. 1, p. 2-18, 2006. DOI: 10.1016/j.catena.2005.10.005
56. WEI, S.C.; ZHANG, X.P.; MCLAUGHLIN, N.B.; CHEN, X.W.; JIA, S.X.; LIANG, A.Z.; Impact of soil water erosion processes on catchment export of soil aggregates and associated SOC. **Geoderma**, v. 294, p. 63-69, 2017. DOI: 10.1016/j.geoderma.2017.01.021
57. WILDNER, W; RAMGRAG, G. E.; LOPES R. C.; IGLESIAS, C. M. F. **Mapa Geológico do Estado do Rio Grande do Sul**. Escala 1:750000. CPRM, Serviço Geológico do Brasil. Porto Alegre, RS. 2006.
58. YAN, L. J.; YU, X. X.; LEI, T.W; ZHANG. Q. W.; QU, L. Q. Effects of transport capacity and erodibility on rill erosion processes: a model study using the Finite Element method. **Geoderma**, v. 146, p. 114-120, 2008. DOI: 10.1016/j.geoderma.2008.05.009
59. ZALÁN, P. V.; WOLFF, S.; ASTOLFI, M. A. M.; VIEIRA, I. S.; CONCEIÇÃO, J. C. J.; APPI, V. T.; NETO, E. V. S.; CERQUEIRA, J. R.; MARQUES, A. The Paraná Basin, Brazil**.** In: LEIGHTON, M. W.; KOLATA, D. R.; OLTZ, D. F.; EIDEL, J. J. **Interior cratonic basins. Tulsa, Okla.**: American Association of Petroleum Geologists, 1990, p. 681-708. (American Association of Petroleum Geologists). Memoir, 51.
60. ZANATTA, F. A. S.; LUPINACCI, C. M.; BOIN, M. N. O uso da terra e alterações do relevo na alta bacia do ribeirão Areia Dourada, Marabá Paulista (SP): um estudo a partir de princípios da Antropogeomorfologia. **Revista Brasileira de Geomorfologia**. v. 16, n.1, p. 3-17, 2015. DOI: 10.20502/rbg.v16i1.560